The Astrophysical Journal, 806:34 (9pp), 2015 June 10 doi:10.1088/0004-637X/806/1/34

A SCENARIO FOR THE FINE STRUCTURES OF SOLAR TYPE IIIb RADIO BURSTS BASED ON ELECTRON CYCLOTRON MASER EMISSION

C. B. Wang[1,2,3]
[1] CAS Key Laboratory of Geospace Environment, School of Earth and Space Science, University of Science and Technology of China, Hefei 230026, Anhui, China; cbwang@ustc.edu.cn
[2] Collaborative Innovation Center of Astronautical Science and Technology, China
[3] Mengcheng National Geophysical Observatory, School of Earth and Space Science, University of Science and Technology of China, Hefei 230026, Anhui, China
Received 2014 July 20; accepted 2015 April 5; published 2015 June 5

ABSTRACT

A scenario based on electron cyclotron maser (ECM) emission is proposed for the fine structures of solar radio emission. It is suggested that under certain conditions modulation of the ratio between the plasma frequency and electron gyro frequency by ultra-low-frequency waves, which is a key parameter for excitation of ECM instability, may lead to the intermittent emission of radio waves. As an example, the explanation for the observed fine-structure components in the solar Type IIIb bursts is discussed in detail. Three primary issues of Type IIIb bursts are addressed: (1) the physical mechanism that results in intermittent emission elements that form a chain in the dynamic spectrum of Type IIIb bursts, (2) the cause of split pairs (or double stria) and triple stria, and (3) why only IIIb–III bursts are observed in the events of fundamental harmonic pair emission whereas IIIb–IIIb or III–IIIb bursts are very rarely observed.

Key words: gamma-ray bursts – magnetohydrodynamics (MHD) – masers – radiation mechanisms: non-thermal – relativistic processes – shock waves – Sun: radio radiation – waves

1. INTRODUCTION

There is a rich variety of fine structures of solar radio emission in the form of wide-band pulsations in emission and absorption with different periods, rapid bursts, and narrow-band patches (Chernov 2011). Specifically, a Type IIIb solar radio burst is a chain of several elementary bursts that appears in dynamic spectra as either single, double, or triple narrow-banded striations, but with an envelope resembling that of a Type III burst (de la Noë & Boischot 1972; de la Noë 1975; Dulk & Suzuki 1980). The study of these fine structures is a key to understanding and verifying the different emission mechanisms of solar radio bursts.

Type III bursts are obviously the most frequent bursts observed from the solar corona. It is generally believed that they are generated by a beam of fast electrons moving along the corona or interplanetary magnetic field line. The plasma emission mechanism is now the most commonly accepted standard model for the generation of Type III bursts, which was first described by Ginzburg & Zheleznyakov (1958) and then refined by a number of researchers (Sturrock 1964; Zheleznyakov & Zaitsev 1970; Smith et al. 1976; Melrose 1980, 1985; Goldman 1983; Robinson & Cairns 1994, 1998a, 1998b, 1998c; Li et al. 2008). In plasma emission theory, it is suggested that streaming electrons first excite Langmuir waves and then part of the energy of the enhanced Langmuir waves is converted into electromagnetic (EM) emissions with frequencies close to the local plasma frequency and its harmonic through nonlinear wave–wave interaction. The differences in existing works are mainly in the details by which the excited Langmuir waves are partly converted to EM waves. In addition, Huang (1998) suggested that Langmuir waves can also be converted directly into EM waves.

Alternatively, a direct emission mechanism based on the electron cyclotron maser (ECM) emission mechanism has been proposed for Type III solar radio bursts (Wu et al. 2002, 2004, 2005; Yoon et al. 2002). Two basic assumptions are made in this ECM emission model. First, it is postulated that density-depleted magnetic flux tubes exist in the corona because in the low-beta corona a small perturbation of the ambient magnetic field in a flux tube can result in considerable density change due to pressure balance (Duncan 1979; Wu et al. 2006). Second, flare-associated streaming electrons possess a velocity distribution with a perpendicular population inversion, which is unstable to ECM instability so that the ordinary (O) mode or extraordinary (X) mode EM waves can be directly amplified with frequencies near the electron gyro frequency or its harmonics in the density-depleted tube. The propagation of amplified radio emission is initially confined within the magnetic flux tube until it arrives at a point where the local exterior cut-off frequency is equal to the exciting wave frequency. On the basis of this model, a number of long-standing issues raised from observations can be resolved simply and self-consistently, such as the existence of fundamental harmonic (F–H) pairs and "structureless" bursts with no visible F–H structure, the same apparent source positions of F- and H-band waves observed at a fixed frequency (McLean 1971; Stewart 1972, 1974; Dulk & Suzuki 1980), the F component being more directive than the H component of F–H pairs (Caroubalos & Steinberg 1974; Dulk & Suzuki 1980; Suzuki & Dulk 1985), and the starting frequency of F waves often being just about one-third to one-fifth that of the H components (Dulk & Suzuki 1980). However, more discussion is needed. An outstanding theoretical issue to be addressed is the explanation of the physical origin of the fine-structure components that occasionally appear in the dynamic spectrum of Type IIIb radio emission.

Type IIIb bursts often consist of a large number of stria bursts but their envelope resembles a Type III burst. Early observational results concerning Type IIIb bursts are reported in Ellis & McCulloch (1967), Ellis (1969), de la Noë & Boischot (1972), de la Noë (1975), and Dulk & Suzuki (1980). In general, there are several types of fine structures such as

double stria bursts, triple stria bursts, fork bursts, etc. The spectral properties of Type IIIb bursts are discussed and reviewed in McLean (1985) and Suzuki & Dulk (1985). Although Type IIIb radio bursts represents merely a fraction of Type III emission events, a theoretical study of such phenomena is essential. In principle, any acceptable theory of Type III emission should be able to explain Type IIIb bursts in the same context.

The commonly held belief about a plasma emission mechanism is that density inhomogeneities in the background plasma create a clumpy distribution of Langmuir waves and are the cause of Type IIIb fine structure (Takakura & Yousef 1975; Melrose 1983; Reid & Ratcliffe 2014). On the other hand, Li et al. (2011a, 2011b) proposed that localized disturbances in the electron temperature and/or ion temperature in the corona may also be responsible for the stria and the Type IIIb bursts. However, the numerical simulation results show that the fine structures are more pronounced for H emission than for F emission (Li et al. 2012). This is inconsistent with the interpretations of many observers that stria bursts occur more often in the F component than in the H component in the case of F–H pair bursts.

Based on the ECM emission scenario, Zhao et al. (2013) recently considered that a linearly polarized homochromous Alfvén wave can modulate the ECM emission process and may be responsible for the fine structure of Type IIIb bursts. In this article, we will propose another scenario for the fine structures of solar radio emission. While we also suggest that under certain conditions ECM emission modulation by ultra-low-frequency (ULF) waves may lead to the intermittent emission of radio waves, a physical process for the modulation that is basically different from that suggested by Zhao et al. (2013). The present scenario is preliminary, but it explains most of the observed features.

The organization of the discussion is as follows. In Section 2 we review briefly the essence of the ECM emission mechanism for Type III bursts which is the basis of the subsequent discussion. Then, in Section 3, a physical model is suggested for Type IIIb emission. Discussion and conclusions are presented in Sections 4 and 5.

2. ELECTRON CYCLOTRON MASER EMISSION OF TYPE III BURSTS

As mentioned in the Introduction, the plasma emission theory is now the most widely known scenario for solar Type III bursts. The ECM emission scenario may be not familiar to some readers, so before discussing the fine structures of solar Type IIIb bursts, it is best to describe briefly the essential points of the ECM emission scenario for normal Type III bursts without fine structures (Wu et al. 2002, 2005; Yoon et al. 2002). The motivation for the ECM emission scenario comes mainly from two observations. (1) Type III bursts are generated by fast electrons associated with solar flares. Most solar flares occur in active regions where the magnetic field is stronger than that elsewhere at the same altitude. Effect of the ambient magnetic field may be important for the emission process. (2) Observations find that waves of the F component and the H component of Type III bursts with the same frequency have coincidental source regions (McLean 1971; Stewart 1972, 1974; Dulk & Suzuki 1980). This implies that the radiation of Type III bursts may be produced in a density-depleted flux tube as first noted by Duncan (1979).

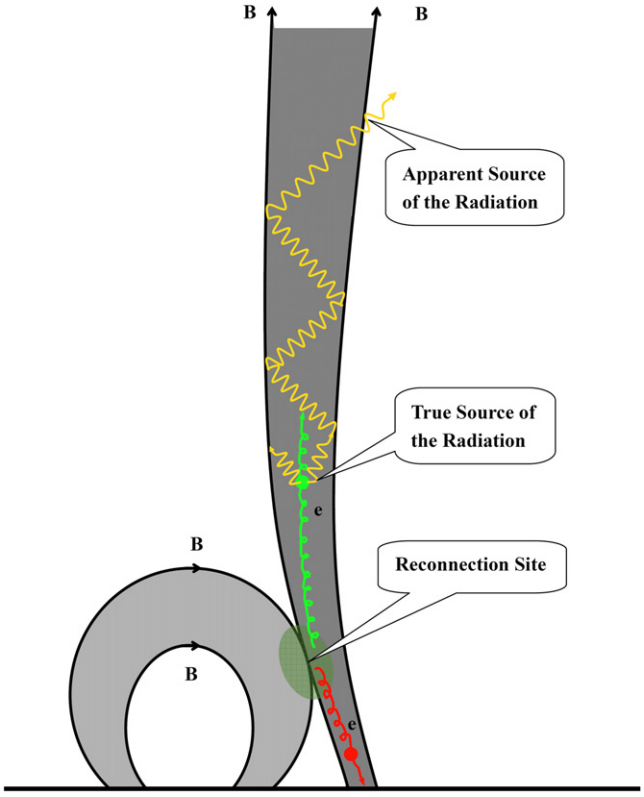

Figure 1. Graphic description summarizing a scenario of Type III bursts based on the electron cyclotron maser emission mechanism.

Figure 1 is a graphic scheme that summarizes one possible ECM emission scenario for solar Type III bursts. We assume that a solar flare occurs somewhere above an active region through magnetic reconnection between a magnetic loop and an open magnetic flux tube in the corona. Energetic electrons are generated during the impulsive phase of the flare. In general, these energetic particles may occur either inside or outside the density-depleted flux tube. We are only interested in those that occur inside an open flux tube with a plasma density that is low enough to ensure the ECM emission is workable. Meanwhile, the energetic electrons may move away from the reconnection site along open field lines in both upward and downward directions. In the present discussion we are interested in the upward-streaming electrons. It is believed that enhanced turbulent Alfvén waves exist pervasively in the solar corona. These waves can pitch-angle scatter the streaming electrons. The pitch-angle scattering accelerates the electrons in the transverse direction and is more effective for fast electrons. As a result, the streaming electrons deform into a crescent-shaped velocity distribution (Wu et al. 2002, 2012) with a perpendicular population inversion, which is unstable to the ECM instability so that the O-mode or X-mode EM waves can be directly amplified with a frequency near the electron gyro frequency or its harmonics in the density-depleted tube. The cut-off frequency of either the X-mode or the O-mode inside the tube is significantly lower than that outside the tube. The true source region, where the radio wave is generated, is inside the tube, and the wave is confined in the tube during propagation if the wave frequency is below the exterior cut-off frequency (thus, the true source region is not observable). This wave cannot leave the tube until it reaches an altitude where the local exterior cut-off frequency becomes lower than

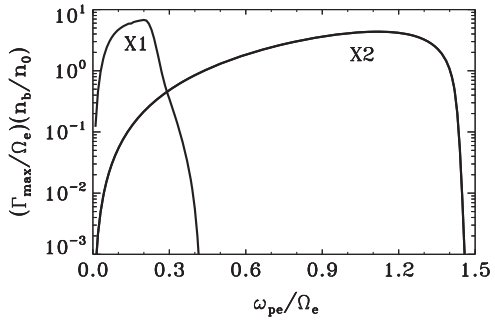

Figure 2. Maximum growth rates of F (fundamental) waves (X1) and H (harmonic) waves (X2) are plotted vs. the ratio ω_{pe}/Ω_e, where n_b and n_0 are the number densities of the energy electrons and ambient electrons, respectively. The velocity distribution of the energy electrons is modeled as $F_b(u_\perp, u_\parallel) = C \exp[-(u_\perp - u_{\perp 0})^2/\alpha^2 - (u_\parallel - u_{\parallel 0})^2/\beta^2]$ with $u_{\perp 0} = u_0 \sin\theta$, $u_{\parallel 0} = u_0 \cos\theta$, $\alpha = 0.1u_{\perp 0}$, $\beta = 0.2u_{\parallel 0}$, $u_0 = 0.3c$, and $\theta = 20°$, and where c is the speed of light. It is seen that amplification of F waves is restricted to a small range of ω_{pe}/Ω_e only.

the wave frequency. We name the region where the wave leaves the density-depleted flux tube as the apparent source region. We consider that the observed source regions of F- and H-waves are actually apparent regions rather than true source regions. Hence, waves with the same frequency would exit at the same altitude regardless the locations of their generation. In addition, we would like to reiterate that Figure 1 is just for illustration purposes. There are a number of solar flare models in the literature (Benz 2008 and references therein).

The details of the ECM instability, the generation mechanism of radio emission suggested above, have already been given in several articles (Wu et al. 2002, 2005; Yoon et al. 2002; Chen et al. 2005), so we will not repeat the discussion here. In principle, both X-mode waves and O-mode waves can be amplified by maser instability. Because O-mode waves have a much lower level of spontaneous emission, their emission level may be insignificant in comparison with that of X-mode waves as discussed in Wu et al. (2002) and Yoon et al. (2002). In the following, we will mainly pay attention to the X-mode waves. In other words, we assume that the X1 mode waves and X2 mode waves with frequencies near the electron gyro frequency and its harmonics correspond to the observed F components and H components of Type III bursts, respectively. Nevertheless, the discussion is also applicable to O-mode waves.

The ratio ω_{pe}/Ω_e (ω_{pe} is the electron plasma frequency and Ω_e is the electron gyro frequency) is a crucial parameter in maser instability. Here we present Figure 2 in which the maximum growth rate is plotted versus the ratio ω_{pe}/Ω_e for the X1 and X2 waves. It is seen from Figure 2 that the X1 waves are amplified by the streaming electrons only if the ratio ω_{pe}/Ω_e falls within the range $0.1 < \omega_{pe}/\Omega_e < 0.4$. Once the ratio ω_{pe}/Ω_e is beyond the upper limit, emission of X1 waves is considerably weakened. However, on the other hand, the condition for X2 waves is $0.1 < \omega_{pe}/\Omega_e < 1.4$, so that the range is much broader. The main reason is that X2 waves have frequencies far above the cut-off frequency and have frequencies near the second harmonic of the gyro frequency.

On the basis of this model, several important issues for Type III bursts raised from observation can be understood naturally. For example,

1. Whether we observe F–H pairs or "structureless" bursts without F–H pairs depends on the frequency ratio ω_{pe}/Ω_e in the flux tube. If the ratio ω_{pe}/Ω_e falls within the range $0.1 < \omega_{pe}/\Omega_e < 0.4$, the burst would be F–H pairs. On the other hand, if ω_{pe}/Ω_e falls within the range $0.4 < \omega_{pe}/\Omega_e < 1.4$, a "structureless" burst would be observed, which is the H component.
2. The observed source region is the apparent region whose altitude is dependent only on the wave frequency. Whether they are F components or H components, waves with the same frequency would exit at the same altitude. Thus, the same apparent source positions of F- and H-band waves would be observed at a fixed frequency.
3. The F waves initially propagate in the oblique direction, while H waves are excited with wavevectors primarily along the nearly perpendicular direction. Moreover, before escaping from the density-depleted tube, F waves must propagate for much longer along the duct than H waves that were generated at the same true source region. Hence, one would expect that F waves are generally more directive than H waves as one can see clearly from the ray-trace results shown by Figure 8 in the paper by Yoon et al. (2002).
4. The emission of F waves starts at an altitude higher than that for H waves, because the excitation of F waves requires a sufficiently large beam momentum (Wu et al. 2005). Hence, one would expect that the ratio of the starting frequencies of H components to those of F components is generally higher than two (Dulk & Suzuki 1980).

3. AN INTERPRETATION OF TYPE IIIB EMISSION

3.1. Basic Consideration

The most conspicuous feature of Type IIIb emission is that in cases of F–H pair emission the fine structure only occurs in the F component (de la Noë & Boischot 1972; Suzuki & Dulk 1985). This outstanding feature implies that in Type IIIb bursts the F component is intermittently suppressed. The key question is what causes the suppression.

As noted before, the ratio ω_{pe}/Ω_e plays a crucial role in the ECM instability. The amplification of the X1 mode requires $0.1 < \omega_{pe}/\Omega_e < 0.4$. Once the ratio is beyond its upper limit, emission of X1 waves is suppressed. On the other hand, the condition for X2 waves is $0.1 < \omega_{pe}/\Omega_e < 1.4$, so that the range is much broader. Evidently, if the density and/or magnetic field vary spatially in a quasi-periodical manner, then the ratio ω_{pe}/Ω_e is expected to vary accordingly. If this variation takes place near the upper limit for X1 waves, say between 0.3 and 0.5, then we expect that the emission of F waves will be on and off spatially when the energetic electrons pass through these regions. (In regions where $0.3 < \omega_{pe}/\Omega_e < 0.4$, the emission is on, but in regions where the plasma has $0.4 < \omega_{pe}/\Omega_e < 0.5$ the emission is off.) On the other hand, H waves are not affected because the instability for X2 waves operates over the range $0.4 < \omega_{pe}/\Omega_e < 0.5$ (or higher). In this case the pair emission appears to be IIIb–III, and no III–IIIb or IIIb–IIIb emission can occur. Of course, the same explanation may also explain the case where Type IIIb bursts consist of only one component. For example, if the ratio ω_{pe}/Ω_e varies around the upper limit for X2 waves, say $\omega_{pe}/\Omega_e \approx 1.4$, then no emission of X1 waves is possible but emission of X2 waves occurs intermittently in

space. As a result we would observe a single-band Type IIIb burst.

We consider that Type IIIb bursts are attributed to the same emission process as Type III bursts but in cases where the radiation is modulated by the density and/or magnetic spatial-variation structures along the path through which the streaming electrons pass. The next question is: What is the cause (or causes) of the spatial structures of the density and/or magnetic field? ULF MHD waves and oscillations, such as magnetosonic waves, Alfvén waves, and sausage modes, may be some of the most probable causes because they exist widely in the solar atmosphere as demonstrated comprehensively both from observations and in theories (Roberts 2000; Aschwanden 2004; Nakariakov & Verwichte 2005; de Moortel & Nakariakov 2012). In the present article we will not elaborate on the theory of the generation of these waves. We just hypothetically postulate that occasionally these waves exist in the source regions of Type IIIb bursts. Our discussion will focus on the consequences that these waves have on the fine structures of Type IIIb bursts.

3.2. Modulation of the Frequency Ratio ω_{pe}/Ω_e

From the above discussion, one can speculate intuitively that the details of the observed fine structures seen in a dynamic spectrum of Type IIIb bursts are determined by the pattern of spatial structures of the ULF waves that modulate the ratio $\omega_{\rm pe}/\Omega_e$ in the source region of the radio emission. In general, spatial variation of the wave field strength as well as the modulated frequency $\omega_{\rm pe}/\Omega_e$ may be different from case to case. For the purpose of illustration and without loss of generality, in this paper, we just discuss three simple cases (namely, modulation of the ratio $\omega_{\rm pe}/\Omega_e$ by a monochromatic wave, by a standing wave, and by two waves that propagate in parallel along the ambient magnetic field) to show what kinds of wave forms can produce the different fine structure patterns observed in Type IIIb bursts.

(a) Modulation of $\omega_{\rm pe}/\Omega_e$ by a monochromatic wave, single stria bursts

Let the ambient magnetic field be in the z direction. Note that $(\omega_{\rm pe}/\Omega_e)_0$ is the frequency ratio in the absence of the wave, and the modulated ratio by a monochromatic ULF wave with parallel propagation can be simply modeled as

$$\frac{\omega_{\rm pe}}{\Omega_e} = \left(\frac{\omega_{\rm pe}}{\Omega_e}\right)_0 \left[1 - \delta_0 \cos\left(\omega t - k_z z\right)\right], \quad (1)$$

where ω and k_z are the wave frequency and the wave number along the ambient magnetic field of the ULF wave, and δ_0 is the amplitude of the modulation factor. Based on the discussion in the pre-subsection, if $(\omega_{\rm pe}/\Omega_e)_0$ just happens to be a marginal value $(\omega_{\rm pe}/\Omega_e)_C$, (e.g., as discussed in the above subsection 3.1), for the excitation of the F waves or H waves so that the emission may be on when

$$\frac{\omega_{\rm pe}}{\Omega_e} = \left(\frac{\omega_{\rm pe}}{\Omega_e}\right)_C \left[1 - \delta_0\right], \quad (2)$$

and the emission may be off when

$$\frac{\omega_{\rm pe}}{\Omega_e} = \left(\frac{\omega_{\rm pe}}{\Omega_e}\right)_C \left[1 + \delta_0\right] \quad (3)$$

where we have made use of the minimum and maximum value of the modulation factor $g_1(t, z) = \cos(\omega t - k_z z)$. Obviously, the present scenario works only if δ_0 is sufficiently large.

If we write $\omega = k_z v_{\rm ph}$ and $t = z/v_b$, where $v_{\rm ph} = \omega/k_z$ is the wave phase speed along the ambient magnetic field and v_b is the beam speed of energetic electrons, then the modulation factor seen by the energetic electrons at different space positions is

$$g_1(t, z) = \cos\left[\left(1 - \frac{v_{\rm ph}}{v_b}\right) k_z z\right] \equiv \cos\left(k_{\rm D} z\right) = \cos\left(\frac{2\pi z}{\lambda_{\rm D}}\right), \quad (4)$$

where $k_{\rm D}$ is the effective wavenumber seen by the streaming electrons due to the Doppler effect and $k_{\rm D} \equiv (1 - v_{\rm ph}/v_b)k_z$. If we assume that the ECM instability operates when $g_1 > 0.7$, we can expect that the Type IIIb bursts would include a number of stria fine structures. In addition, each element of the fine structures has only one striation in this condition, compared to the split-pair or triple stria bursts which include two or three striations in each element and will be discussed in (b).

(b) Modulation of $\omega_{\rm pe}/\Omega_e$ by a standing wave or two waves, double and triple stria bursts.

First, we study the case where there is a standing wave. Occasionally, low-frequency MHD waves may be produced high above the source region of Type IIIb bursts. Since both the ambient magnetic field and density change with altitude, the Alfvén speed varies too. As the wave propagates to a lower altitude, it experiences a higher Alfvén speed (and thus higher wave phase speed). This can be seen from the following relation

$$v_{\rm A} = \sqrt{\frac{m_e}{m_p}} \frac{c}{\omega_{\rm pe}/\Omega_e} \quad (5)$$

where m_e and m_p are the masses of electrons and protons and c and $v_{\rm A}$ are the speed of light and the Alfvén speed. Inside the flux tube, the ratio $\omega_{\rm pe}/\Omega_e$ generally decreases with decreasing altitude, so the Alfvén speed increases with deceasing altitude. This means the refractive index in the z direction decreases. As a result, we consider that the descending-propagation MHD wave may be reflected at a low altitude of the source region of the radio emission. For example, An et al. (1989) have demonstrated that transient Alfvén waves propagating from a region with low Alfvén speed to a region with higher Alfvén speed can be reflected and even trapped in a cavity. On the other hand, it is commonly believed that there are standing waves in a corona loop due to wave reflection at the two footpoints of the loop (e.g., Wang 2011; Li et al. 2013 and references therein). If we assume the descending waves have a narrow frequency spectrum so that they may be represented by one wave, and in addition, the descending wave continues for a sufficiently long time period, say many ion gyro periods, and finally, that there is no dissipation process during the reflection, then the superposition of the two wave fields will form a standing wave. One can model the modulated frequency ratio by the standing wave as

$$\frac{\omega_{\rm pe}}{\Omega_e} = \left(\frac{\omega_{\rm pe}}{\Omega_e}\right)_0 \left\{1 - \delta_0\left[\cos\left(\omega t + k_z z\right) + \cos\left(\omega t - k_z z + \varphi_0\right)\right]\right\} \quad (6)$$

where ω and k_z are the wave frequency and wavenumber and φ_0 is the wave phase difference between the ascending wave

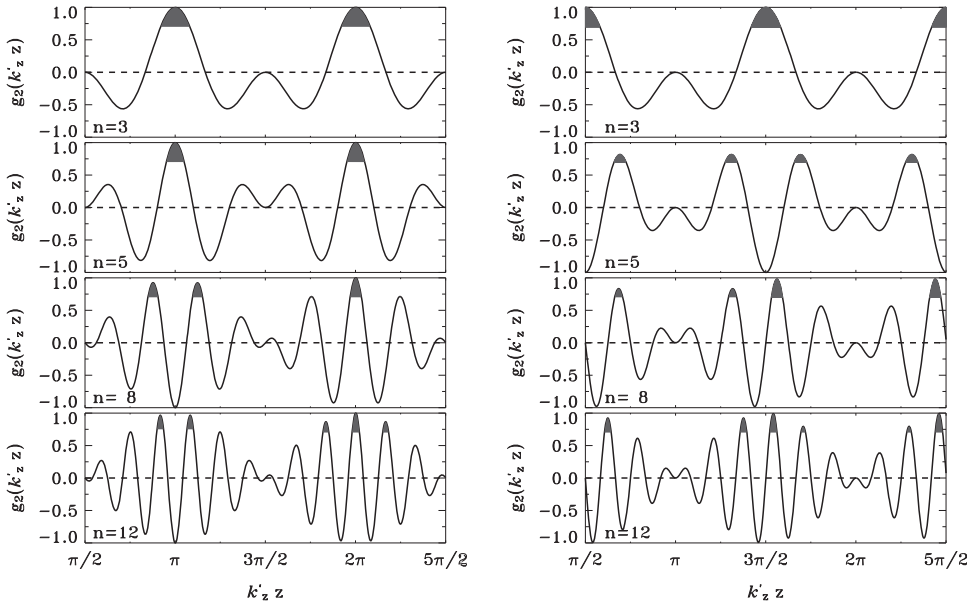

Figure 3. Modulation factor of the standing wave plotted as a function of $k_z' z$ for several values of n. The left and right panels are for the results with a wave phase constant of $\phi_0 = 0$ and $\phi_0 = \pi/2$, respectively. For illustration purposes, it is assumed that the maser instability operates when $g_2 > 0.7$. It is seen that in the case of $n = 3$ or 5, single stria elements may occur, whereas in the case of $n = 8$ and 12, double and/or triple stria bursts may happen.

and descending wave. An important assumption in obtaining Equation (6) is that the wave field retains more or less the same form when it returns to the same height.

Similarly, let $\omega = k_z v_{\rm ph}$ and $t = z/v_b$, where the modulation factor seen by the energy electrons has the following form:

$$g_2(t, z) = \cos\left(k_z' + \varphi_0/2\right)\cos\left(k_z - \varphi_0/2\right),$$
$$k_z' \equiv k_z(v_{\rm ph}/v_b) \tag{7}$$

The function g_2 consists of two parts: one is an envelope and the other is a much shorter wavelength wave. For convenience we define the envelope as the E wave and the latter wave as the S wave. If the S-wave has a wavelength λ_S and the E wave has a wavelength λ_E, then we define

$$n \equiv \frac{\lambda_E}{\lambda_S} = \frac{v_b}{v_{\rm ph}}. \tag{8}$$

In Figure 3 we plot the numerical result of g_2 in terms of $k_z' z$. Several values of n are considered. It is seen that the characteristics change as the ratio n varies. In the case of $n = 3{,}5$ with $\phi_0 = 0$ in each of the intervals $\pi/2 \leqslant k_z' z \leqslant 3\pi/2$ and $3\pi/2 \leqslant k_z' z \leqslant 5\pi/2$, the function g_2 has one peak close to unity. The feature changes as n increases. For example, when n is 8, there may be one or two peaks depending upon the threshold values of instability. In the case of $n = 12$, we see that in the interval $\pi/2 \leqslant k_z' z \leqslant 3\pi/2$ or $3\pi/2 \leqslant k_z' z \leqslant 5\pi/2$, there are two peaks or three peaks close to 1. The results with $\phi_0 = \pi/2$ are similar to that of $\phi_0 = 0$. We suggest that the twin peaks represent the double stria bursts while one or three peaks may explain single or triple stria bursts.

When the beam speed is much larger than the wave phase speed, for example, the Alfvén speed, Type IIIb would show double or triple stria bursts. On the other hand, there will be only single stria bursts. The upper limit of the frequency ratio $\omega_{\rm pe}/\Omega_e$ for F-wave and H-wave emission is about 0.4 and 1.4, and the corresponding Alfvén speed is about 0.059 and 0.017 c, respectively. This indicates that a much higher value of electron beam speed is necessary to produce double or triple stria bursts in the F component than for the H component when modulation by a standing Alfvén-like wave is the cause of Type IIIb bursts.

Second, we consider the case where there are two waves propagating upward along the ambient magnetic field. The transient spatial variation of the modulated ratio can be modeled as

$$\frac{\omega_{\rm pe}}{\Omega_e} = \left(\frac{\omega_{\rm pe}}{\Omega_e}\right)_0 \Big\{1 - \big[\delta_0 \cos\left(\omega_1 t - k_{z1} z\right)$$
$$+ \delta_0 \cos\left(\omega_2 t - k_{z2} z + \varphi_0\right)\big]\Big\}. \tag{9}$$

Here we simply assumed two waves with the same wave amplitude with frequencies and wavenumbers of (ω_1, k_{z1}) and (ω_2, k_{z2}), respectively. φ_0 is the difference between their wave phase constants. Note

$$k_1' = \frac{1}{2}\left(1 - \frac{v_{\rm ph}}{v_b}\right)\left(k_{z1} + k_{z2}\right), \tag{10}$$

$$k_2' = \frac{1}{2}\left(1 - \frac{v_{\rm ph}}{v_b}\right)\left(k_{z1} - k_{z2}\right) > 0, \tag{11}$$

the modulated frequency ratio seen by the streaming electrons is

$$\frac{\omega_{\rm pe}}{\Omega_e} = \left(\frac{\omega_{\rm pe}}{\Omega_e}\right)_0 \big[1 - 2\delta_0 \cos\left(k_1' z + \varphi_0/2\right)$$
$$\times \cos\left(k_2' z - \varphi_0/2\right)\big]. \tag{12}$$

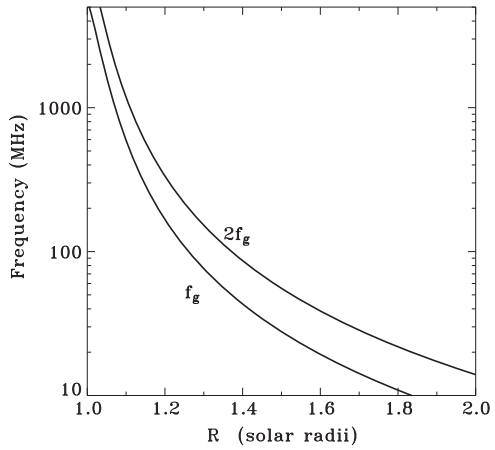

Figure 4. Variation of the electron gyro frequency and its harmonics with altitude in the density-depleted tube, where the magnetic field is modeled by a unipolar magnetic field of a sunspot-field model with a maximum field strength of 2000 Gauss at the center of the spot on the photosphere and a spot radius of 0.05 $R_\odot$.

and the modulation factor is written as

$$g_3(t, z) \equiv \cos\left(k_1' z + \varphi_0/2\right)\cos\left(k_2' z - \varphi_0/2\right) \quad (13)$$

The factor g_3 has the same functional form as that of g_2, which also consists of two parts: one is an envelope and the other is a shorter-wavelength wave. Now, the ratio between the wavelength of the E wave and that of the S wave is defined as

$$n \equiv \frac{\lambda_E}{\lambda_S} = \frac{k_{z1}'}{k_{z2}'} = \frac{k_{z1} + k_{z2}}{k_{z1} - k_{z2}} \quad (14)$$

Thus, one can expect that the modulation of the frequency ratio ω_{pe}/Ω_e by two monochromatic waves also can produce single, double, or triple stria bursts depending on the difference in their wave numbers or frequencies.

4. DISCUSSION

We will first discuss the mean frequency interval between the adjacent elements in a chain of stria bursts where an element may include one striation for a single stria burst, two striations for a split-pair burst, or three striations for a triple burst. Based on our scenario, this frequency interval is determined by two parameters, namely the gradient of the ambient magnetic strength with altitude and the wavelength of MHD waves producing the modulation. In this discussion, the magnetic field in an active region is modeled by a unipolar magnetic field of a sunspot-field model with a maximum field strength of 2000 Gauss at the center of the spot on the photosphere and a spot radius of 0.05 $R_\odot$ (Zheleznyakov 1970; Yoon et al. 2002). Figure 4 shows the variation of the electron gyro frequency and its harmonic with altitude in units of solar radius.

The discussion of a chain of single stria bursts is relatively simple, without loss of generality, so we mainly pay attention to the split-pair bursts and triple stria bursts in this section. According to our scenario the frequency interval between the adjacent elements is that between the adjacent peaks of the E waves. If the E wave has a parallel wavelength λ_E at an altitude H where the gyro frequency is $f_g = \Omega_e/2\pi$, then at altitude $H + \lambda_E$, the gyro frequency changes to $f_g - \Delta f_g$. On the basis on the cyclotron maser scenario, the frequency interval between two elements, Δf_E, should be $\Delta f_g/2$ (or Δf_g) for F waves (or H waves). If we *know* n and if we denote the frequency gap in a double or triple stria burst by Δf_S, then we find $\Delta f_S = 2\,\Delta f_E/n$. Here we remark that in the present theory the gap Δf_S is the same for either double stria or triple stria bursts. This finding seems to be consistent with the observational results discussed in McLean (1985).

Let us consider two cases separately: (i) the single-band Type IIIb emission and (ii) the IIIb–III pair emission.

(i) Single Component Type IIIb Bursts

In this case, the waves are assumed to be X-mode harmonic (X2) waves. On the basis of the proposed scenario the observed frequencies should be $2f_g$. Since the commonly observed Type IIIb bursts have frequencies in the range of 20–60 MHz (de la Noë & Boischot 1972; de la Noë 1975), the corresponding altitudes are in the range of 1.5–2.0 solar radii as shown in Figure 4. Making use of these results we can calculate Δf_S, which is defined earlier, versus altitude if a wavelength λ_S of the S wave is assumed. In the present discussion we consider several wavelengths of the S wave. These are postulated to be 200, 500, 1000, and 5000 km. The purpose is to see which wavelength would yield the most reasonable results in comparison with observations. Using the scheme stated in the preceding section we estimate the frequency gap Δf_S in a double or triple stria as a function of altitude. The results are plotted in Figures 5(a) and (b) (solid lines). In Figure 5(a), Δf_S is expressed as a function of altitude, whereas in Figure 5(b), it is shown versus the emission frequency. We can further calculate Δf_E (for a given value of $n = \lambda_E/\lambda_S$), the frequency interval between (envelope) elements, which are also shown in Figures 5(a) and (b) (dashed lines) by assuming $n = 8$.

From the obtained results we draw the following conclusions:

1. The frequency interval Δf_S or Δf_E increases with emission frequency. For example, if we choose to consider the case in which the MHD wavelength is 1000 km, we find that at an emission frequency of 20 MHz the frequency gap Δf_S is 70 kHz while at an emission frequency of 60 MHz the frequency gap Δf_S is about 350 kHz. The corresponding value of Δf_E varies from 0.56 MHz at 20 MHz to 2.9 MHz at 60 MHz.
2. According to the present theory, the occurrence of triple stria bursts requires a relatively high λ_E/λ_S ratio. When the frequency ratio ω_{pe}/Ω_e is modulated by a standing wave, this happens either with a high beam speed or at high altitudes where the wave phase speeds as well as the radiation frequencies are low.

(ii) IIIb–III Pair Emission

We now move on to discussing F–H pair emission in which under certain conditions the F waves may have structured emission whereas the H waves are like a normal Type III burst. The observed frequencies of the fine structures should be f_g. The altitudes for the emission with frequencies in the range 20–60 MHz are in the range 1.3– 1.6 solar radii as shown in Figure 4.

Figures 6(a) and (b) show the variation of the frequency interval Δf_E (dashed lines) and the frequency gap Δf_S (solid lines) with the altitude and with the emission frequency, respectively. In this case we find that most of the conclusions obtained in the above subsection still hold. As the radiation frequency increases, the frequency interval of both the E wave

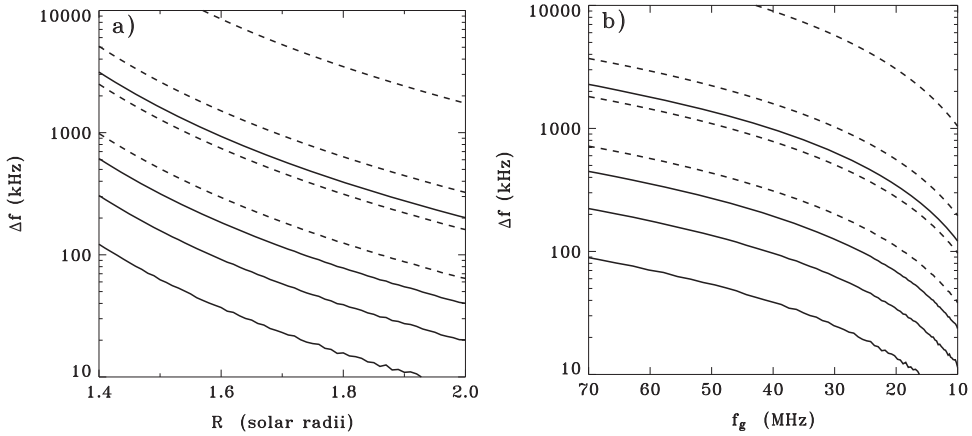

Figure 5. (a) Numerical results of the frequency interval Δf between elements and striations for the case of single-component Type IIIb bursts are shown as a function of altitude. The solid curves represent the interval Δf_S in the fine structure while the dash curves are Δf_E for the envelope wave. Several wavelengths of the S wave are considered. The wavelength of the E wave is assumed to be eight times the value of the S wave. Curves from the lower-left corner to the upper-right corner represent the results with wavelengths of $\lambda_S = 200$, 500, 1000, and 5000 km, respectively. (b) The same results presented in (a) are shown as functions of emission frequency. This is done on the basis of the cyclotron maser scenario from which the altitude is converted to radiation frequency.

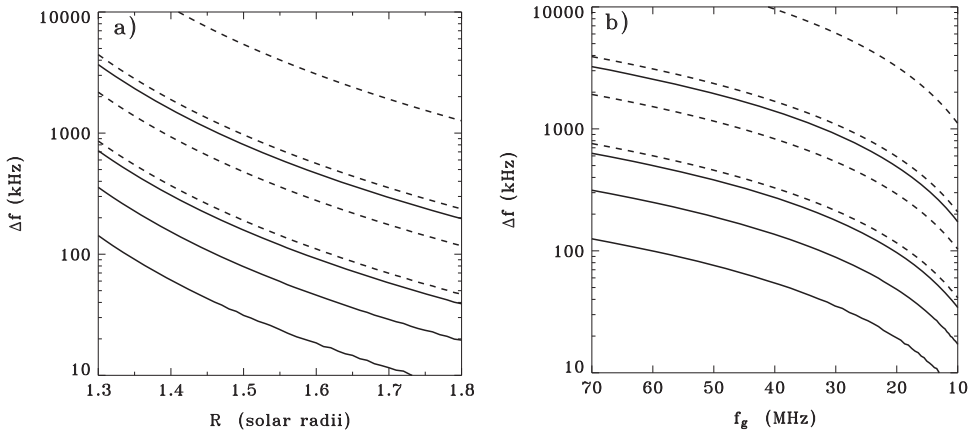

Figure 6. (a) Numerical results of frequency interval Δf between elements and striations for the IIIb–III case are shown as function of altitude. The solid curves represent the interval Δf_S in the fine structure while the dash curves are Δf_E for the envelope wave. Several wavelengths of the S wave are considered. The wavelength of the E wave is assumed to be eight times the value of the S wave. Curves from the lower-left corner to the upper-right corner represent the results with wavelengths of $\lambda_S = 200$, 500, 1000, and 5000 km, respectively. (b) The same results presented in (a) are shown as functions of emission frequency. This is also done as in Figure 5(b) by converting the altitude to radiation frequency.

and the S wave increases as well. It is found that, in the case in which the wavelength λ_S is 1000 km, the frequency interval Δf_S (or Δf_E) at emission frequencies of 20 and 60 MHz are about 100 kHz (or 0.6 MHz) and 500 kHz (or 3.1 MHz), respectively. The frequency intervals are slightly larger than those for single-component Type IIIb bursts because the altitude of the true source region of the F wave is lower than that of the H wave with the same emission frequency, and the gradient of the magnetic field strength increases with decreasing altitude.

In addition, observations show that the fine structures occur most at low frequencies or more often at high altitudes. A qualitative discussion for this observation is as follows. According to the present scenario, two necessary conditions are needed to produce fine structure. First, the ambient frequency ratio $(\omega_{pe}/\Omega_e)_0$ without MHD waves is near its upper limit for the excitation of ECM instability. This limit is approached more often at high altitude since the ratio $(\omega_{pe}/\Omega_e)_0$ is generally increasing with increasing altitude in the true source region of the emission in the flux tube. Second, the amplitude of the MHD waves is large enough to modulate the frequency ratio ω_{pe}/Ω_e in a wide range so that the radio emission can be switched on and off spatially. Since both the ambient magnetic field strength and the plasma density decrease with increasing altitude, their values can be disturbed more easily at high altitudes than at lower altitudes. For example, assuming an Alfvén wave propagating upward along the flux tube from an altitude H_1 to altitude H_2 without dissipation ($H_2 > H_1$), it is easy to demonstrate from the conservation of wave energy that

$$\frac{\delta B_2^2/B_{0,2}^2}{\delta B_1^2/B_{0,1}^2} = \frac{v_{A1}}{v_{A2}}\frac{B_{0,1}}{B_{0,2}} \tag{15}$$

where δB_i, $B_{0,i}$, and v_{Ai} are the wave amplitude, the ambient magnetic field strength, and the Alfvén speed, respectively. Index "$i = 1, 2$ " represents parameters at altitudes H_1 and H_2. Both the ambient magnetic field strength and the Alfvén speed generally decrease with increasing altitude in the flux tube. Thus, the higher the altitude is, the larger the relative

perturbation of the magnetic field strength $\delta B^2/B_0^2$ is expected to be.

5. CONCLUSIONS

To summarize, in this paper we propose a possible scenario for the fine structures of Type IIIb bursts based on the ECM emission theory of solar Type III radio bursts. The essence of the scenario is that the presence of enhanced MHD waves in the source region of radio emission, the normal Type III emission is modulated by the spatial structure of the density and/or magnetic field associated with the ULF MHD waves. The details are discussed in Section 3.

The conclusions drawn from the present theory are consistent with observations. Among them, the following points deserve attention.

1. The proposed scenario is able to resolve the issue of why only IIIb–III but no IIIb–IIIb or III–IIIb cases are observed in F–H pair emission.
2. The scenario can explain the occurrence of split-pair (or double stria) bursts and triple stria bursts. Moreover, the scenario also predicts that in a triple stria burst the fine structure is symmetric with respect to the middle striae.
3. In general, fine-structure components of Type IIIb emission occur in high altitudes where the radiation frequencies are low. The frequency separation of striae in a given burst increases with increasing radiation frequency (Ellis 1969; de la Noë 1975).
4. Concerning the polarization of Type IIIb bursts, X-mode waves are assumed in the above discussion. However, the scenario is also applicable for O-mode waves since there is an upper limit of the frequency ratio ω_{pe}/Ω_e for O-mode emission. That is, the fundamental O1 mode can be excited in the condition $0.1 < \omega_{pe}/\Omega_e < 1.0$, while the condition for the harmonic O2 mode is $0.1 < \omega_{pe}/\Omega_e < 2.0$ which is much broader. One of the essential conclusions, which is in agreement with observations as reported in Ellis (1969), de la Noë & Boischot (1972), and de la Noë (1975), is that the elements of a pair or a triplet stria burst are always polarized in the same sense.

For illustration purposes we present Figure 7 in which we depict a calculated dynamic spectrum for the case of single-component Type IIIb emission. This figure is calculated based on the scheme used in Wu et al. (2002); the wavelength of the MHD wave is assumed to be 1000 km. In this figure we show a chain of split-pair and triple stria bursts.

The preliminary results presented in this paper are encouraging for the ECM scenario of Type III bursts, but more discussion is still needed in the future. For example, observation of the Type III burst polarization in the literature seems to favor the O mode, although there are uncertainties (the difficulty stems from the fact that there is no directional measurement of the polarity of the magnetic field in the corona source region where the radiation originates). Regarding this point, the recent work by Wu et al. (2012) deserves attention. It is found that the growth rate of O-mode waves in the ECM instability may be significantly influenced by intrinsic Alfvén turbulence in the solar corona through modifying the resonant wave–particle interaction (Wu et al. 2012; Wu 2014; Wu et al. 2014). Furthermore, Zhao et al. (2013) applied this theory to explain the fine structures of Type IIIb bursts by assuming the modulation is caused by a linearly polarized monochromatic

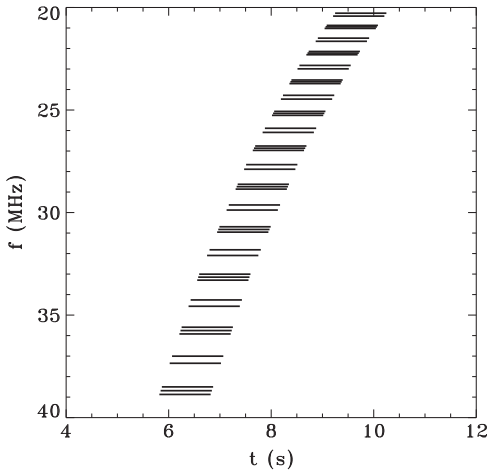

Figure 7. Numerically created dynamic spectrum for the case of single-component Type IIIb emission. Elements of fine structures with split-pair and triple stria bursts are illustrated. The time duration is arbitrarily taken to be one second.

Alfvén wave. The numerical results show that these effects mainly enhance the growth rate of the fundamental O1 mode. This seems to favor the idea that the F component is an O-mode one while the H component is an X-mode one. However, observations indicate that the polarization of Type IIIb bursts does not differ significantly from that of normal F–H pairs, and the sense of polarization of F and H radiation is invariably the same (Dulk & Suzuki 1980). Thus, we do not consider the influence of the ULF waves on the wave–particle resonant interaction in the present study. While we also suggest that the fine structures are according to intermittent emission of radio waves modulated by ULF MHD waves, the physical process for their modulation is basically different from that discussed in the paper by Zhao et al. (2013).

This scenario may also help us to understand other types of solar radio bursts with fine structures such as zebra bursts (Kuijpers et al. 1980; Ning et al. 2000; Chen et al. 2011; Yu et al. 2013), which will be discussed in the future. Finally, as pointed out by the referee, the main point of the present paper, generation of Type IIIb fine structures in terms of emission modulated by standing (or slowing traveling) waves in the magnetic field, does not depend on a specific emission mechanism.

The research was supported by the National Science Foundation of China grants 41174123, 41421063, WK2080000031, and WK2080000077, the Chinese Academy of Sciences grants KZCX2-YW-QN512 and KZZD-EW-01, and the Fundamental Research Funds for the Central Universities under grant WK2080000031.

REFERENCES

An, C.-H., Musielak, Z. E., Moore, R. L., & Suess, S. T. 1989, ApJ, 345, 597
Aschwanden, M. J. 2004, Physics of the Solar Corona (Berlin: Springer)
Benz, A. O. 2008, LRSP, 5, 1
Caroubalos, C., & Steinberg, J. L. 1974, A&A, 32, 245
Chen, B., Bastian, T. S., Gary, D. E., & Jing, J. 2011, ApJ, 736, 64
Chen, X. P., Wang, C. B., & Zhou, G. C. 2005, AcPSn, 54, 3221
Chernov, G. P. 2011, Fine Strucuture of Solar Radio Bursts (Heidelberg, Dordrecht, London, New York: Springer)
de la Noë, J. 1975, A&A, 43, 201

de la Noë, J., & Boischot, A. 1972, A&A, 20, 55
de Moortel, I., & Nakariakov, V. M. 2012, RSPTA, 370, 3193
Dulk, G. A., & Suzuki, S. 1980, A&A, 88, 203
Duncan, R. A. 1979, SoPh, 63, 389
Ellis, G. R. A. 1969, AuJPh, 22, 177
Ellis, G. R. A., & McCulloch, P. M. 1967, AuJPh, 20, 583
Ginzburg, V. L., & Zheleznyakov, V. V. 1958, SvA, 2, 653
Goldman, M. V. 1983, SoPh, 89, 403
Huang, G. L. 1998, ApJ, 498, 877
Kuijpers, J. 1980, in Proc. IAU Symp. No. 86, Radio Physics of the Sun, ed. M. R. Kundu & T. E. Gergely (Dordrecht: Reidel), 341
Li, B., Habbal, S. R., & Chen, Y. 2013, ApJ, 767, 169
Li, B., Rosbinson, R. A., & Cairns, I. H. 2008, JGR, 113, A10101
Li, B., Rosbinson, R. A., & Cairns, I. H. 2011a, ApJ, 730, 20
Li, B., Rosbinson, R. A., & Cairns, I. H. 2011b, ApJ, 730, 21
Li, B., Rosbinson, R. A., & Cairns, I. H. 2012, SoPh, 279, 173
McLean, D. J. 1971, AuJPh, 24, 201
McLean, D. J. 1985, in Solar RadioPhysics, ed. D. J. McLean & N. R. Labrum (Cambridge: Cambridge Univ. Press), 37
Melrose, D. B. 1980, SSRv, 26, 3
Melrose, D. B. 1983, SoPh, 87, 359
Melrose, D. B. 1985, in Solar RadioPhysics, ed. D. J. McLean & N. R. Labrum (Cambridge: Cambridge Univ. Press), 177
Nakariakov, V. M., & Verwichte, E. 2005, LRSP, 2, 3
Ning, Z., Fu, Q., & Lu, Q. 2000, A&A, 364, 853
Reid, H. A. S., & Ratcliffie, H. 2014, RAA, 14, 773
Roberts, B. 2000, SoPh, 193, 139
Robinson, P. A., & Cairns, I. H. 1994, SoPh, 154, 335
Robinson, P. A., & Cairns, I. H. 1998a, SoPh, 181, 363
Robinson, P. A., & Cairns, I. H. 1998b, SoPh, 181, 395
Robinson, P. A., & Cairns, I. H. 1998c, SoPh, 181, 429
Smith, R. A., Goldstein, M. L., & Papadopoulos, K. 1976, SoPh, 46, 515
Stewart, R. T. 1972, PASAu, 2, 100
Stewart, R. T. 1974, SoPh, 39, 451
Sturrock, P. A. 1964, NASSP, 50, 357
Suzuki, S., & Dulk, G. A. 1985, in Solar RadioPhysics, ed. D. J. McLean & N. R. Labrum (Cambridge: Cambridge Univ. Press), 289
Takakura, T., & Yousef, S. 1975, SoPh, 40, 421
Wang, T. 2011, SSRv, 158, 397
Wu, C. S., Reiner, M. J., Yoon, P. H., Zheng, H. N., & Wang, S. 2004, ApJ, 605, 503
Wu, C. S., Wang, C. B., & Lu, Q. M. 2006, SoPh, 235, 317
Wu, C. S., Wang, C. B., Wu, D. J., & Lee, K. H. 2012, PhPl, 19, 082902
Wu, C. S., Wang, C. B., Yoon, P. H., Zheng, H. N., & Wang, S. 2002, ApJ, 575, 1094
Wu, C. S., Wang, C. B., Zhou, G. C., Wang, S., & Yoon, P. H. 2005, ApJ, 621, 1129
Wu, D. J. 2014, PhPl, 21, 064506
Wu, D. J., Chen, L., Zhao, G. Q., & Tang, J. F. 2014, A&A, 566, A138
Yoon, P. H., Wang, C. B., & Wu, C. S. 2002, ApJ, 576, 552
Yu, S., Nakariakov, V. M., Selzer, L. A., Tan, B., & Yan, Y. 2013, ApJ, 777, 159
Zhao, G. Q., Chen, L., & Wu, D. J. 2013, ApJ, 779, 31
Zheleznyakov, V. V. 1970, Radio Emission of the Sun and Planets (New York: Pergamon)
Zheleznyakov, V. V., & Zaitsev, V. V. 1970, SvA, 14, 47